Stochastic Parameterizations for Improving the Estimation of Channelized Reservoirs in an Assisted History Matching Context

Bogdan SEBACHER

***Abstract*—In this paper, we introduce two novel parameterizations of channelized facies fields generated with the multipoint geostatistics simulation model (MPS) in combination with a training image. In a previous study, we suggested calculating, from the ensemble, the facies probability fields and linking it, marginally, with the standard Gaussian variables by the means of normal score transform. The conditional expected value of the Gaussian density was used to parameterize the facies fields. As a consequence, the sampling from the Gaussian distribution is discrete and bimodal. Here, we extend this parameterization in two directions. First, we parameterize the facies fields by random sampling from the conditional Gaussian distribution, independently for each grid cell. The second idea is to draw samples from the conditional distribution using the same random seed for each grid cell within each ensemble member, but different seeds across the ensemble members. This procedure, by comparison with the original parametrization, would preserve the spatial dependence structure within each ensemble member while increasing the variability between the ensemble members. Both parameterizations have the property that, marginally, they sample correctly from the standard Gaussian distribution. We compare the behavior of the parameterizations within a history matching process, assimilating production data. We will show that the new parameterizations estimate better the channel position than the older parameterization. In addition, at the end of the assimilation process, one of the parameterizations preserves the geological characteristics of the prior. We have used the iterative adaptive Gaussian mixture filter (IAGM) for history matching because the IAGM is suited for highly nonlinear problems and has a resampling step that allows us to use the already existing technique of resampling from the training image using updated probability fields.**

***Index Terms*—Channelized Reservoirs, Parameterization, History Matching, Iterative Adaptive Gaussian Mixture filter, Uncertainty Quantification.**

I. INTRODUCTION

The estimation of channelized reservoirs conditioned to production data has been extensively studied in the reservoir engineering community. This problem poses difficulties from the beginning when a reliable geological simulation model has to be chosen to simulate facies fields that exhibit channelized geometry. It is well known that the truncated Gaussian simulation model (TPS, [8], [22-23]) fails in this matter and, to our knowledge, two geological simulation models have been proved suitable to simulate channelized reservoirs: the multi-point geostatistical simulation (MPS, [1]) models and the object-based simulation models ([3], [15]). Once the geological simulation model is chosen, there are two options to estimate the position of the channels conditioned to production data: either the distribution of the permeability (or a parameterization of it) is estimated and, subsequently, if necessary, the channel positions are inferred from it, or a parameterization of the facies fields is defined, which permits the estimation of the channels directly.

From the first category, in [21] is proposed a method to project the permeability field into a multi-dimensional feature-kernel space, and using the kernel-principal component analysis (K-PCA), they performed a parameterization in this space. The model parameters from the feature space were coupled with the ensemble Kalman filter ([7]) for history matching of the production data. In [5], is presented a comparison of the estimations of permeability field of two-facies channelized reservoirs. The author has used the parameterization of the permeability field defined by the principal component analysis (PCA) and K-PCA in combination with an ensemble smoother with multiple data assimilation (ES-MDA, [6]) as the history matching (HM) method. A parameterization of the permeability field with the singular value decomposition (SVD) method has been introduced in [32], where the authors present a comparison between Randomized Maximum Likelihood (RML) and EnKF. In [17], the K-SVD methodology defines a set of sparse geologic scenarios that are used for estimating the permeability field within an inverse modeling procedure. This methodology was further modified in [16] for estimating the channels using a regularization term in the objective function of the HM method. In [26] the channelized facies fields were estimated with a low-dimensional parameterization derived from the high order singular value decomposition (HOSVD). In [12], the permeability field is parameterized using a basis obtained by applying the discrete cosine transform (DCT) and, the parameters updated in the EnKF framework were the coefficients of the DCT transformation. A modified version of the DCT method has been introduced in [36] by combining it with the ES-MDA for permeability estimation of channelized reservoirs. After the updated step of the history matching, a post-processing optimization-based procedure was employed for the reconstruction of the facies field. In [14], DCT was coupled with a normal score transformation for a reliable permeability estimation of the channelized reservoir using EnKF as the HM method. In [35], the permeability field is estimated using an iterative ensemble smoother and production data measurements

B. SEBACHER is associate professor of Military Technical Academy "Ferdinand I", department of Applied Computer Science (email: bogdan.sebacher@mta.ro)

Digital Object Identifier 10.32754/JMT.2022.1.01

followed by a projection onto a discrete space with a post-processing technique based on wavelet transformation. In [11], is proposed a methodology named the probability conditioning method (PCM). Here the probability field of the channel is inferred from the estimated permeability field and further used to condition the MPS algorithm to it. Consequently, the updated channelized fields are derived by random sampling from the training image with the MPS, conditioned to the estimated probability field. In [37], the authors use the normal-score transform to project the permeability field onto a standard Gaussian space. After the updating, the permeability field is, then, reconstructed based on the inverse of the normal-score transformation.

In the second category, the estimation of the channel borders carries out with the aid of a parameterization of the facies fields. In [19], the authors propose a parameterization using the distance from the grid-cell to the border of the channel. If the grid-cell is inside, the distance function is positive and, if the cell is outside, the distance is negative. These distances are further updated within an EnKF process, assimilating production data and conditioned to some statistical measures to keep the continuity of the channels. The level set method ([4]) is used in [20] for the parameterization and estimation of the channel distribution in 2D and 3D reservoirs. In [10], parameterization is defined inside the MPS simulation method. The authors considered the uniform numbers used in the facies simulation as the parameters to be estimated in the HM process. The principal component analysis (PCA) is also used to parameterize channelized reservoirs. In [33], the authors implemented an optimization-PCA method to parameterize non-Gaussian complex models and, in [34], the parameterization was coupled with the randomized maximum likelihood (RML) method for estimation and uncertainty quantification of the channels.

In this study, we focus on the second category using the MPS as a geological simulation model in combination with a channelized training image. In [24-25, 28], we introduced a parameterization bridging the MPS with the truncated Gaussian and pluri-Gaussian simulation models. This parameterization was successfully applied for estimation and uncertainty quantification of the complex 3D-channelized reservoir of the Brugge field. In [2], an object-based geological simulation model is used for generating the prior facies fields, and this shows that our framework is more general than just using an MPS model with a training image. The parameterization consists of defining some random fields marginally Gaussian, which, in combination with a truncation map simulate the same facies fields with those previously obtained from the training image. Here we propose two parameterizations based on the same idea, but the random fields are different. In [24-25], the marginally Gaussian random fields were defined by the conditional mean of a standard normal variable. In this study, we explore two directions: the first idea is to randomly sample from the conditional distribution using different random seeds for each grid-cell within each ensemble member, and the second idea is to randomly sample from the conditional distribution using a unique random seed for all the grid cells of an ensemble member, but different seeds across ensemble members. In the original parameterization ([24-25]), the choice of the conditional mean is deterministic and, this could cause a deficiency in randomness and provide a smaller uncertainty. The characterization of the prior is crucial in any assisted history matching (AHM) procedure and, consequently, we wanted to explore if, by increasing the prior uncertainty of the parameter field, we obtain better results in terms of estimation and/or data match and prediction. We have chosen two sampling techniques, one that ensures a controlled dependence structure and one that gives a conditional independence structure. We compare these parameterizations within an assisted history matching process using the iterative adaptive Gaussian mixture filter (IAGM, [29]), assimilating production data. The comparison has two main directions: to quantify the impact of the stochastic forcing on the history matching of geological properties and to study the stochastic forcing on the predictive power of the models. The use of the IAGM is suitable here because the IAGM works well for highly nonlinear problems and has a resampling step that allows us to use the technique of resampling with MPS from the training image conditioned to updated probability fields ([18]). The resampling is necessary because after an assimilation cycle, the channelized geometry may be broken, and the resampling repositioning the channel structure. The permeability and porosity are kept constant within each facies type and not considered uncertain as in [9] and [27] because we are interested in the estimation of facies boundaries.

In the following sections, we introduce the parameterizations, present the IAGM with its customized implementation for our problem and a case study where we perform the comparison. The paper ends with conclusions.

II. PARAMETERIZATIONS

The geological simulation model used for generating the initial ensembles is the Single Normal Equation Simulation Model (SNESIM, [31]), where the training image that represents the geological concept of the channelized reservoir is presented in Fig. 1. In this section, we start by presenting the parameterization proposed in [24] and, we extend the sampling framework in two directions.

Let us consider an ensemble of n_e channelized reservoirs, simulated with SNESIM from the training image using as constraints only the global facies proportions, on a square reservoir domain with 100×100 grid cells. We calculate, from this ensemble, the probability field of channel occurrence (Fig. 2) which marginally means the calculation of a value p^j representing the probability that grid cell j is inside a channel of the reservoir domain.

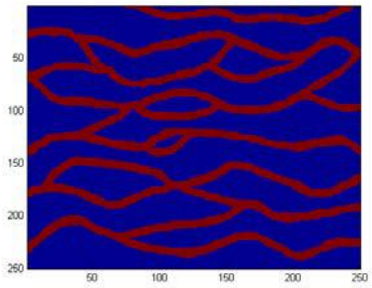

Figure 1. The training image [31]

 Digital Object Identifier 10.32754/JMT.2022.1.01

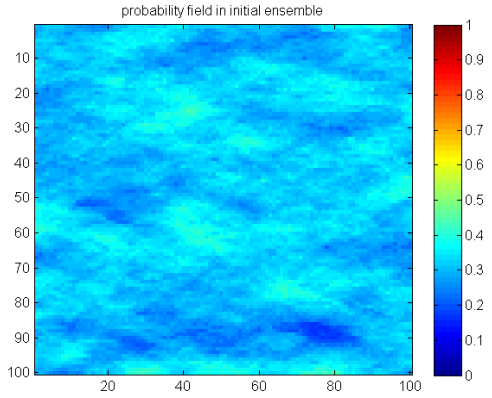

Figure 2. The probability field of the channel

At each grid cell j we consider a discrete random variable denoted $f\_distrib$ with the discrete probability distribution described in (1).

$$f\_distrib^{j} \sim \begin{pmatrix} Channel & Non-channel \\ p^{j} & 1-p^{j} \end{pmatrix} \tag{1}$$

The idea is to link this discrete random variable with a standard normal variable and, the easiest way is to apply the normal score transform. Consequently, we calculate the cumulative distribution of this random variable and define the threshold $\alpha^{j} = \Phi^{-1}\left(p^{j}\right)$ in the Gaussian space, where function Φ is the standard Gaussian cumulative distribution function, $\Phi(x) = \frac{1}{\sqrt{2\pi}} \int_{-\infty}^{x} \mathrm{e}^{-\frac{u^2}{2}} du$.

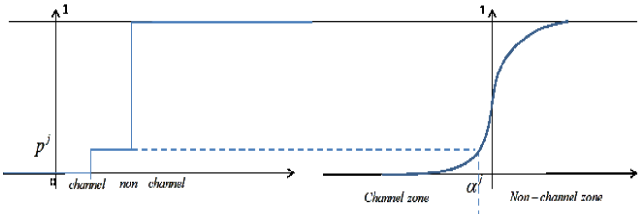

Figure 3. The normal score transform

The threshold α^{j} splits the real axis in two intervals $\left(-\infty, \alpha^{j}\right]$ and $\left(\alpha^{j}, \infty\right)$ corresponding to the channel and non-channel respectively (Fig. 3). Fig. 4 shows the spatial distribution of thresholds α in the reservoir domain. We can clearly see a strong spatial structure similar to the structure of the probability field of channel (Fig. 2). The spatial distribution of the probability field of channel (Fig. 2) is the result of a finite size ensemble, and asymptotically (if n_e goes to infinity) is constant and equal with the prior global channel proportion used as input in the SNESIM. However, all of the ensemble members share the same multi-point statistics and consequently, the probability field (which is a mean), inherits a certain spatial dependence from the ensemble. We will transfer this spatial dependence structure in the parameterizations that will be further defined.

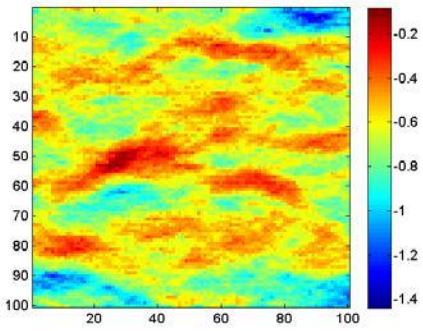

Figure 4. Threshold field

The parameterization is performed in the multi-dimensional real space $\mathbb{R}^{n}$, where N is the dimension of the reservoir domain (number of the grid cells, in our case 10000). For each ensemble member i (a facies field) we define a parameter field on the reservoir domain, denoted θ_i.

In the next section, we present three alternatives for the parameterization with different levels of randomness.

A. Gravity Center (GC) parameterization

Here we present the idea from [24] parameterizing the facies field using the gravity centers of the $\left(-\infty, \alpha^{j}\right]$ and $\left(\alpha^{j}, \infty\right)$ with respect to the standard Gaussian density $\phi(x) = \frac{1}{\sqrt{2\pi}} \mathrm{e}^{-\frac{x^2}{2}}$. Consequently, for the ensemble member i we define at the grid cell j the value of parameter field θ_i^{j} as

$$\theta_i^{j} = \begin{cases} E\left(X \middle| X \le \alpha^{j}\right) = -\dfrac{\phi\left(\alpha^{j}\right)}{\Phi\left(\alpha^{j}\right)} \\ \qquad if\ cell\ j \in channel \\ E\left(X \middle| X > \alpha^{j}\right) = \dfrac{\phi\left(\alpha^{j}\right)}{1-\Phi\left(\alpha^{j}\right)} \\ \qquad if\ cell\ j \notin channel \end{cases}, \tag{2}$$

where X is a random variable following a standard normal distribution.

B. Random Mapping (RM) parameterization

The first new parameterization introduced in this article is defined by sampling from the marginal conditional Gaussian distribution, but using the same seed for each grid cell within an ensemble member. The initial step is to calculate (in (3) and (4)) the cumulative distribution function (cdf) of the conditional Gaussian distributions $\left(X \middle| X \le \alpha^{j}\right)$ and $\left(X \middle| X > \alpha^{j}\right)$

$$F_{X|X\le\alpha^{j}} = \begin{cases} \dfrac{\Phi\left(\alpha^{j}\right)}{\Phi\left(\alpha^{j}\right)}, & if\ x \le \alpha^{j} \\ 1, & if\ x \le \alpha^{j} \end{cases} \tag{3}$$

$$F_{X|X>\alpha^j} = \begin{cases} 0\,, & \text{if } x \le \alpha^j \\ \dfrac{\Phi(x) - \Phi(\alpha^j)}{1 - \Phi(\alpha^j)}, & \text{if } x \le \alpha^j \end{cases} \quad (4)$$

For sampling from a random variable Y with known cumulative distribution function F_Y we use the probability integral transform. Then, if $\tilde{y}$ is a random sample from Y, $F_Y(\tilde{y})$ is a sample from a uniformly distributed variable on $[0,1]$. Consequently, for each ensemble member i we draw a random sample (seed) y from the uniform distribution $U(0,1)$ and, after solving the equations: $F_{(X|X\le\alpha^j)} = y$ and $F_{(X|X>\alpha^j)} = y$, we find the following solutions, $x = \Phi^{-1}\left(y_i \cdot \Phi(\alpha^j)\right)$ and $x = \Phi^{-1}\left(\Phi(\alpha^j) + y_i \cdot \left(1 - \Phi(\alpha^j)\right)\right)$. These values are random samples from the conditional Gaussian $(X|X \le \alpha^j)$ and $(X|X > \alpha^j)$. Consequently, using a unique seed y_i for each grid cell j of the reservoir domain, we define the parameter field θ associated with member i as follows

$$\theta_i^j = \begin{cases} \Phi^{-1}\left(y_i \cdot \Phi(\alpha^j)\right) \\ \qquad \text{if } j \in channel \\ \Phi^{-1}\left(\Phi(\alpha^j) + y_i \cdot \left(1 - \Phi(\alpha^j)\right)\right) \\ \qquad \text{if } j \notin channel \end{cases} \quad (5)$$

C. Fully Random Mapping (FRM) parameterization

The second new parameterization introduced in this article is based on the idea of defining the parameter field θ by a random sampling from a conditional Gaussian distribution. The sampling is done randomly for each ensemble member and for each grid cell of the reservoir domain. Consequently, for ensemble member i we define at grid cell j the value of the parameter field θ_i^j as

$$\theta_i^j = \begin{cases} \text{random sampling from } (X|X \le \alpha^j) \\ \qquad \text{if } j \in channel \\ \text{random sampling from } (X|X < \alpha^j) \\ \qquad \text{if } j \notin channel \end{cases} \quad (6)$$

In the light of the parameterization with random mapping, the parameter field from (6) could be written as,

$$\theta_i^j = \begin{cases} \Phi^{-1}\left(y_i^j \cdot \Phi(\alpha^j)\right) \\ \qquad \text{if } j \in channel \\ \Phi^{-1}\left(\Phi(\alpha^j) + y_i^j \cdot \left(1 - \Phi(\alpha^j)\right)\right) \\ \qquad \text{if } j \notin channel \end{cases} \quad (7)$$

This means that for each ensemble member i and for each grid cell j we are using a different seed y_i^j for sampling from conditional Gaussian distributions $(X|X \le \alpha^j)$ and $(X|X > \alpha^j)$.

III. Comparison of the Parameterizations before History Matching

In Fig. 5 we present two members of the ensemble of channelized reservoirs (first column) and the associated parameter fields. In the second column we show the parameter fields calculated with the parameterization with gravity center (GC), in the third column the parameter fields calculated with fully random mapping (FRM) and in the fourth column the parameter fields calculated with the random mapping (RM). From this figure, we see that the FRM-parameterization destroys any possible spatial structure inherited from the probability field of channel (Fig. 2); inside of the channels or outside of the channels we find values with no spatial correlation. This is not happening for the other two parameterizations, inside of each body of facies the values of the parameter field have a spatial correlation structure inherited from the probability field of channel. However, for the case of RM-parameterization (last column), we observe a higher variability than the one observed for the GC-parameterization (second column) because the ranges of the parameter field are different for different ensemble members.

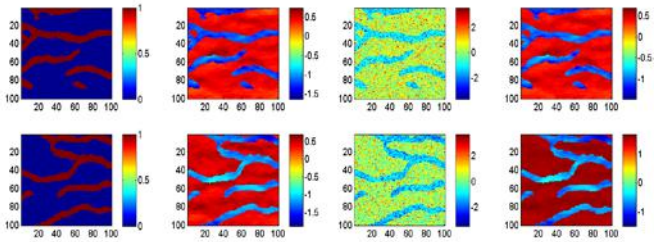

Figure 5. The facies fields and the associated parameter fields

In Fig. 6 we show the mean of the parameter field calculated from the ensemble for all parameterizations. For the GC-parameterization the mean is a zero uniform field by construction ([24]), whereas the other two means are not zeros, but their values are close to zero. The mean field of parameter θ, calculated from the ensemble generated with the FRM-parameterization is a field with values randomly distributed over domain whilst in the mean field of the RM-parameterization one can clearly see a spatial correlation similarly with those seen in the threshold field (Fig. 4).

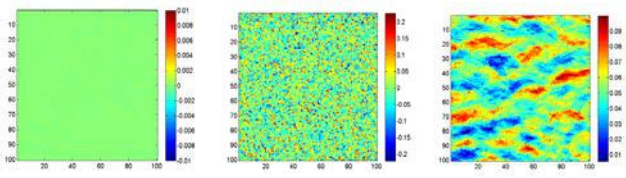

(a) Gravity Center (b) Fully Random Mapping (c) Random Mapping

Figure 6. The mean of the parameter field for all parameterizations

In Fig. 7 we present the histograms of the values of parameter fields $\{\theta_i\}_{i=1}^{n_e}$. In the first line the histogram is calculated from the ensemble of values of the first cell of the reservoir domain. In the second line we present the histogram of values of the all cells of the first ensemble member.

 Digital Object Identifier 10.32754/JMT.2022.1.01

For the parameterization with gravity centers, we approximate (marginally) the standard Gaussian distribution with a bimodal distribution (Fig. 7, first row, middle picture)) which is a bad approximation. The last two parameterizations sample much better from the Gaussian distribution (the left and right positions of the first row of Fig. 7). If we calculate the histogram of the parameter field from ensemble member 1 we observe a bimodal behavior of the parameterization with gravity centers and with random mapping whilst the fully random mapping yields a Gaussian distribution (second row of Fig. 7).

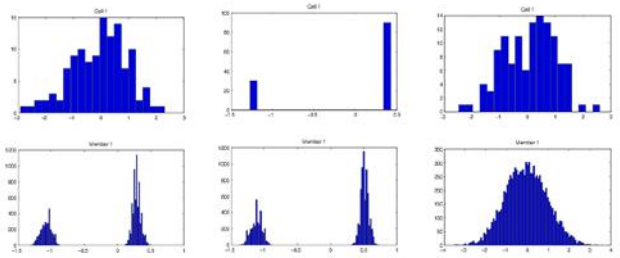

(a) Random Mapping (b) Gravity Center (c) Fully Random Mapping

Figure 7. The histograms of parameter field values in all parameterizations

Before the history matching, all the parameterizations define parameter fields which by truncation yield exactly the same facies fields. However, the sampling from the conditional Gaussian distribution was performed gradually in terms of randomness. This implies different levels of uncertainty in the prior ensemble of parameter fields. In the following, we will test if this prior uncertainty influences the estimation process of the channels or the data match and prediction when we employ the parameterizations in the history matching.

IV. The Iterative Adaptive Gaussian Mixture Filter (IAGM)

The iterative adaptive Gaussian mixture filter (IAGM) is the iterative version of the adaptive Gaussian mixture filter (AGM, [30]) developed for improving the AGM for nonlinear models ([29]). In the AGM the uncertainty of the system is represented by an ensemble of possible states and each ensemble member (particle) has an associated likelihood weight. Initially all ensemble members have the same weight (equally weighted), $\widehat{W_j} = \frac{1}{n_e}, j \in \overline{1, n_e}$, as in the ensemble Kalman filter (EnKF). In our case, the ensemble of parameter fields consists of the fields $\left\{\theta^i\right\}_{i=1}^{n_e}$ and we denote by G_t, the function that maps the parameters to observations. We augment our state vector with these variables. Hence, our ensemble state vector $X_t^i, i \in \overline{1, n_e}$ is given by

$$X_t^i = \begin{bmatrix} \theta_{t,i}^T & G_t\left(\theta_{t,i}\right)^T \end{bmatrix}^T, i = 1 \ldots n_e. \tag{8}$$

This augmentation allows us to construct, for each assimilation time *t*, a binary matrix H_t so that $Y_t = H_t X_t + \varepsilon_t$, where ε_t follows a Gaussian distribution with mean 0 and known covariance matrix R_t. That is, the measurement is a linear function of our augmented state vector with additive Gaussian white noise. The measurements used in this study are the bottom hole pressures taken at the injection wells, the oil and water rates taken at the production wells. The dynamical variables (the pressure and saturation fields) are not included in the state vector as we have chosen to re-run the simulator from time zero after each assimilation.

Let be C_t the sample covariance matrix of $\left\{X_t\right\}_{i=1}^{n_e}$ calculated based on the weighted ensemble mean

$$\overline{X_t} = \sum_{i=1}^{n_e} \widehat{W_t^i} X_t^i. \tag{9}$$

At each assimilation time, the augmented state vector is updated in the AGM (and IAGM) for each $i \in \overline{1, n_e}$ as

$$\begin{aligned} \widehat{X_t^i} = X_t^i + C_t H_t^T \left(H_t C_t H_t^T + h^{-2} R_t\right)^{-1} \\ \cdot \left(y_t - H_t X_t^i + \varepsilon_t^i\right) \end{aligned} \tag{10}$$

here ε_t is a sample from the Gaussian measurement error distribution $N\left(0; R_t\right)$.

The update is similar with the standard EnKF, the only difference is the scaling h^{-2} of the measurement error covariance matrix R_t. In other words the linear update is dampened, where the dampening factor h^{-2} $\left(h \in [0,1]\right)$ is the bandwidth of the Gaussian mixture ([30]). For *h* equal to 1 we get the standard EnKF update.

In addition to a linear update, importance weights are derived from the Gaussian mixture and updated sequentially as

$$\begin{aligned} \overline{W}_t^i = \widehat{W}_{t-1}^i \phi\left(y_t - H_t X_t^i, H_t C_t H_t^T + R_t\right) \\ W_t^i = \frac{\overline{W}_t^i}{\sum_{j=1}^{n_e} \overline{W}_t^j} \end{aligned} \tag{11}$$

Here, the function $\phi\left(x - \mu, C\right)$ represents multivariate Gaussian density with mean μ and covariance matrix C. To avoid filter degeneracy that occurs in high dimensions and complex systems a weight interpolation is introduced,

$$\widehat{W}_t^i = \alpha_t W_t^i + \left(1 - \alpha_t\right) n_e^{-1}, \alpha_t \in [0,1] \tag{12}$$

where

$$\alpha_t = n_e^{-1} \left(\sum_{i=1}^{n_e} \left(W_t^i\right)^2 \right)^{-1}. \tag{13}$$

For details of the AGM we refer to [29]. A resampling and reweighting step in the algorithm before rerunning AGM is discussed in [29].

A. Reconstruction of the facies fields

After the assimilation of the data, the values of parameter field θ are changing according to (10) (the updated parameter field is denoted here by θ^u). Using the new values we update the facies fields on a cell by cell basis:

"For each ensemble member $i \in \overline{1, n_e}$ *and for each grid cell* $j \in \overline{1, N}$ *if* $\theta_i^{u,j} \le \alpha_j$ *we assign the channel to the grid cell and if* $\theta_i^{u,j} > \alpha_j$ *we assign the non-channel facies type."*

This truncation will project a continuous field into a discrete field (as in the truncated Gaussian method).

B. Resampling in IAGM

The SNESIM has incorporated the tau model ([13], [18]) which enables integration of the probabilities coming from soft data and the training image. Usually, the probability maps used as soft data are coming from seismic interpretations, but here, we adopt the procedure from [11] but using the probability fields of the facies calculated after an iteration of IAGM. The tau model depends on two weights, denoted τ_1 and τ_2, that calibrates the geological concept (the training image) with the probability fields. In this study, the weights used are both equal to 1, which correspond to the equal importance assigned to the training image and weighted probability map respectively.

After one complete assimilation cycle, new weighted probability fields (of the channel and non-channel) are constructed from the updated ensemble of channelized reservoirs,

$$p_k^j = \sum_{i=1}^{n_e} \widehat{W}_t^i Ind_k^{i,j}, k = channel, non-channel \quad (14)$$

where

$$Ind_k^{i,j} = \begin{cases} 1 & if \quad cell\ j \in facies\ type\ k \\ 0 & if \quad cell\ j \notin facies\ type\ k \end{cases}. \quad (15)$$

Here the indices *i* represent the ensemble member and *j* are indicative of the grid cell and denote the time. Using the tau model, we generate a new ensemble of channelized reservoirs conditioning the training image to the weighted probability fields of the facies types. The resampling step of the IAGM repositions the facies geometry and this is one of the reasons for using this AHM method. After each iteration, we evaluate the ensemble from the channel geometry and data match perspective and decide if it is necessary to proceed with another iteration. After a finite number of iterations, the updated ensemble of facies fields remain geologically realistic and provide, in addition, a good data match.

The algorithm of one complete assimilation cycle with the AGM can be summarized as follows,

1. Generate an ensemble of n_e channelized reservoirs from the training image and the weighted probability field of facies (at the initial step each probability field is constant and equal to the global proportion of the facies type).
2. Calculate the parameter fields θ_i for each $i \in \overline{1, n_e}$.
3. Construct the state vector $X^i, i \in \overline{1, n_e}$ as in (8) associating equal weights of $\frac{1}{n_e}$ to each ensemble member and set the dampening parameter *h*.
4. For each assimilation time *t* do:
   a. Run the simulator from time 0 to the time *t*, populating first the facies fields with petrophysical properties.
   b. At the assimilation time *t*, assimilate the data, updating the state vector $\widehat{X_t^i} = X_t^{i,up}, i \in \overline{1, n_e}$ according to (10) and the weights according to (11), (12) and (13).
   c. Reconstruct the updated facies fields using the updated parameters $\theta_{t,i}^{up}$.
5. Calculate the updated probability fields of facies based on the updated ensemble of facies fields and the updated weights according to (14).

V. Case Study

The reservoir model used for testing has a square shape with 10000 grid cells having dimension of each grid cell $30 \times 30 \times 20$ ft. We design the reservoir as 13-spot water flooding black oil model, having four injection wells and nine production wells (Fig. 8). The reservoir is initially filled with oil at a constant uniform saturation of 0.8 (the connate water saturation is 0.2) and with a uniform pressure of 5000 psi in every grid cell. The producers work under constant bottom-hole pressure (BHP) with a value of 3000 psi and the injectors operate at 3500 STB/D constrained by a maximum BHP of 100000 psi. The measurements were obtained through forward simulation of a synthetic model presented as the "reference" which was randomly sampled from the same training image using SNESIM (Fig. 1).

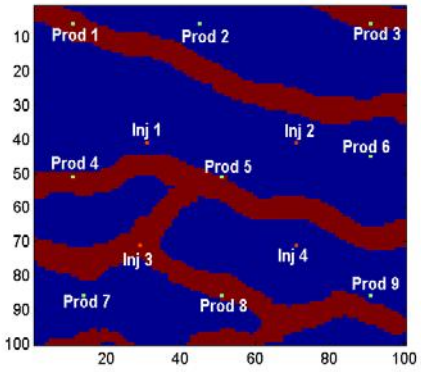

Figure 8. The reference field

The measurement errors of the production data are Gaussian distribution with 0 mean and standard deviations of 70 STB/D for water rates (WR) and oil rates (OR) at the producers, and 200 psi for BHP at the injectors. We use these values for the generation of noisy observations from the reference model. In addition, the distribution is used to perturb the observations of production data in the analysis step of the HM process. Water injection starts from the first day and continues thereafter for 351 days of production. We assimilate data at 60-day intervals resulting in a total of 6 assimilation steps. The permeability values were set at 9 mD and 1 mD for the channel facies type and the non-channel facies type, respectively, while the porosity of both facies types is set to 0.2 and considered as known. The ensemble size is set to $n_e = 120$.

 Digital Object Identifier 10.32754/JMT.2022.1.01

In Fig. 9, we present the probability fields of the channel in the initial (resampled, in even rows) and updated ensembles (odd rows) for three iterations with IAGM, for all parameterizations: gravity centers (GC), random mapping (RM), and fully random mapping (FRM). In all experiments, the initial ensemble of facies fields (channelized reservoirs) is the same and is shown in Fig. 9. Analyzing the last row of Fig. 9, where the probability fields of the channel in the last iteration are presented, we observe that all parameterization provides a reasonable estimation of the true position of the channels in the reservoir domain (Fig. 8).

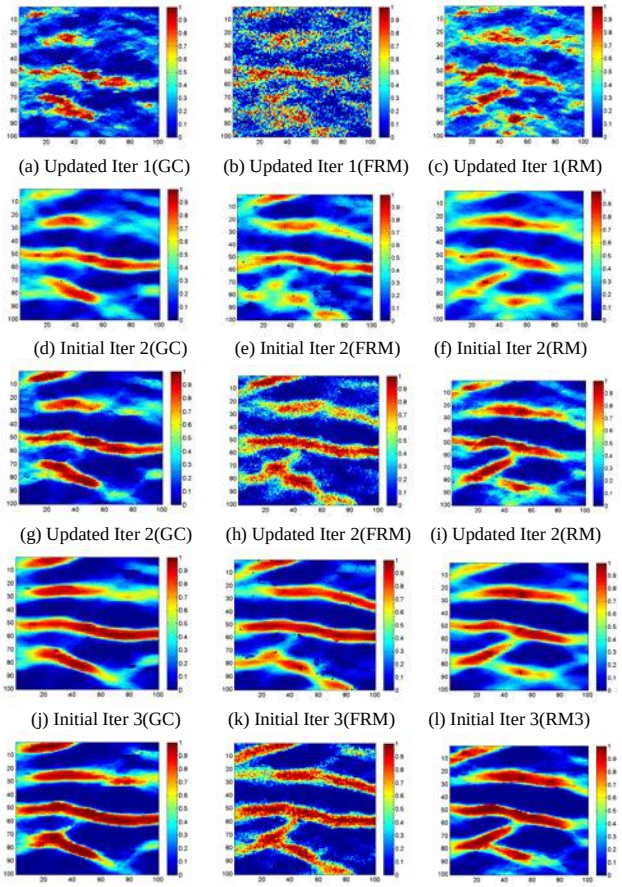

Figure 9. The probability fields of channel for all parameterizations (GC-gravity center, RM-random mapping, FRM-fully random mapping)

However, there is still a difference regarding the connection between the two channels situated at the bottom part of the reservoir. RM-parameterization was able to detect a connection between these channels while the parameterization with gravity centers was not able to do it well. Injector no. 3 is situated at the intersection between the main bottom channel with the small channel and the rates of producers no. 8 and no. 5 could be influenced by the injector no. 3. If we look in Fig. 9 ((a),(b),(c)), where we show the updated probability fields of the channel after the first iteration, we can see that the GC-parameterization does not detect a connection between the channels whereas the other two parameterizations are detecting it. Moreover, in this example, the GC-parameterization detects mainly horizontal connections between wells, but the other two parameterizations were able to detect a vertical flow from the injector no. 3, and this even from the first iteration.

In our opinion, this fact is due to the prior ensemble of the parameter field. The higher variability of the prior ensemble in the RM-parameterization is due to the use of different seeds for each ensemble member when sampling from the condition Gaussian distribution. The FRM-parameterization is also able to estimate this small channel that links the two horizontal channels located at the bottom of the reservoir, which supports our claim and the variability of its prior ensemble is even higher. However, from Fig. 9 we observe that the lack of the spatial correlation of the parameter fields of the FRM-parameterization affects the probability fields of the channel in the sense that the channel position is diffusely estimated (Fig. 9, sub-figures (b), (h), (n)).

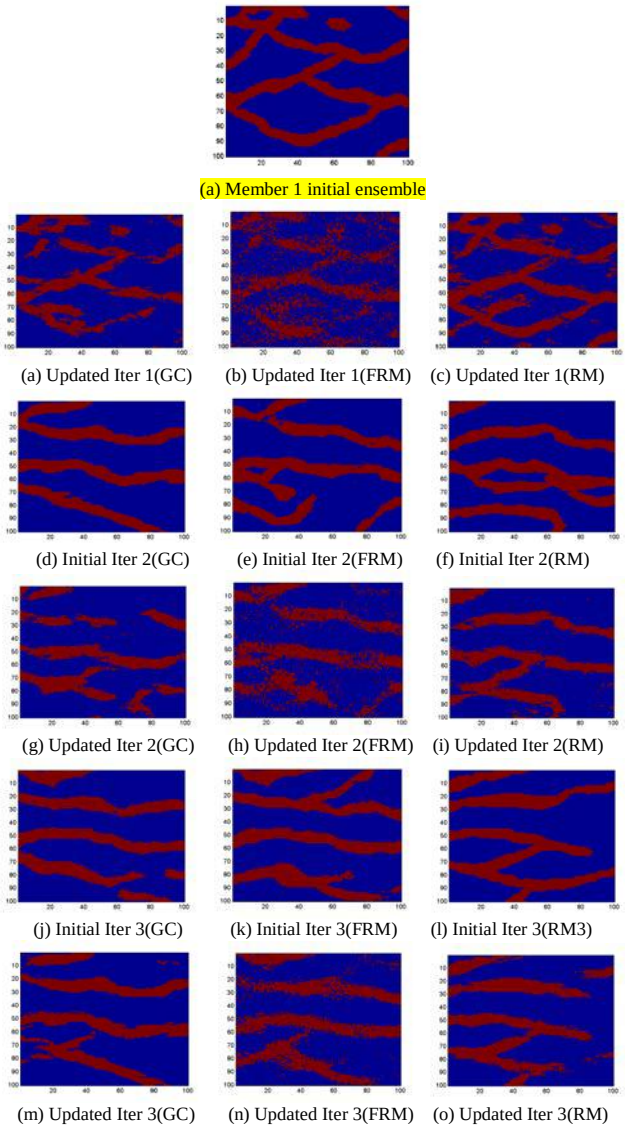

Figure 10. Member 1 in initial and updated ensembles for all parameterizations (GC-gravity center, FRM-fully random mapping, RM-random mapping)

This behavior is very clear especially at the first iteration (Fig. 9, (b)). In addition, the variogram structure (two-point statistics) of the parameter fields defined by GC-parameterization and RM-parameterization improve the estimation of the channels after the first iteration; the probability fields of the channel for both parameterizations exhibit areas better shaped than the probability field of the channel from the FRM-parameterization.

The probability fields of the channels are calculated from ensembles of facies fields either generated with SNESIM or the result of estimation with the IAGM. They only present possible positions of the channel in the field and do not offer

any information of the geological plausibility of the channel fields. In order to quantify the uncertainty of the channel distribution, we have to look at the facies fields. In Fig. 10 we show the evolution of the first member of the ensembles during the experiments. Initially, it presents a nice channelized structure (sub-figure (a)) because it is the result of a simulation from the training image. We can also see how the structure is regained after each resampling for all parameterizations (odd rows).

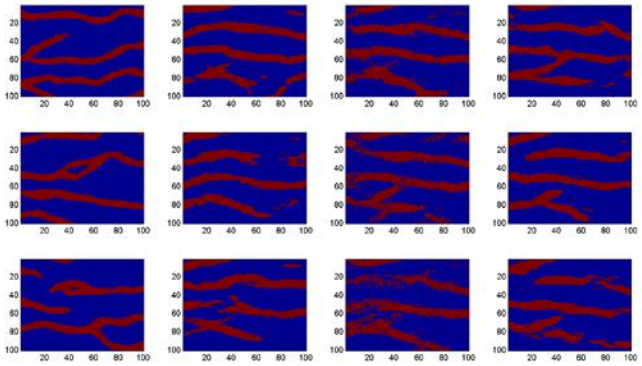

Figure 11. Three facies fields in prior and updated ensembles

The channelized structure is broken differently after the assimilation steps during the history matching. For the GC-parameterizations and RM-parameterization, the updated member still have continuous bodies, whilst for the FRM-parameterization, the updated member is far from the geological concept presented by the training image, even after the third iteration. This can also be seen in Fig. 11, where are shown three members in the prior ensemble (first column) and the updated ensembles after the third iteration (GC-parameterization in the second column, FRM-parameterization in the third column, and RM-parameterization in the fourth column). We believe the reason is the lack of spatial dependence of the parameter fields defined by the FRM. However, the facies fields obtained with this parameterization look better with iterations and are close to the estimation with gravity centers (sub-figure (o) vs sub-figure (n) and (p)). We performed three iterations with IAGM, taking the stopping criterion from [24]. We have stopped the iterative process when the updated facies fields look reasonably from a geological plausibility perspective. Of course, this raises the question of whether if for different parameterizations one should use different iteration numbers. The number three seems to be a good choice for GC-parameterization and RM-parameterization but for the FRM-parameterization seems that it needs more iterations. However, increasing the number of iterations for this parameterization would not increase the quality of the estimation substantially. We continue the comparison by presenting the water rates at all the production wells in all the experiments for 651 days split into two periods: the assimilation period (from 0 to 351) and the prediction period from (351 to 651 days). In Fig. 12 is presented the water rates profiles at the wells in the initial ensemble. Figure 13 shows the water production rates for the gravity center parameterization and, in Fig. 14 and Fig. 15 are presented the water production rates for the FRM-parameterization and RM-parameterization respectively. From the figures, we note that it is difficult to see any distinct difference in HM and prediction between the three parameterizations. This is not a surprise since all parameterizations match the data modifying the channel position in the field on a grid cell basis and all have a sufficient degree of freedom to do it.

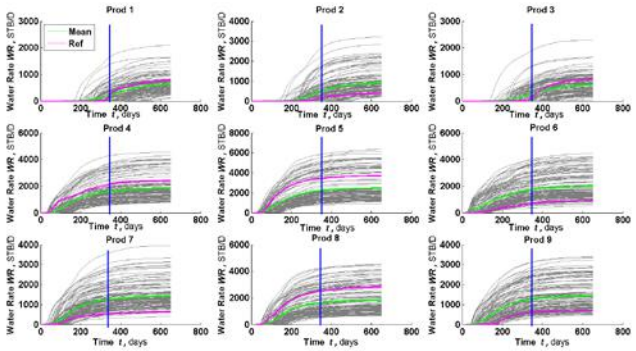

Figure 12. Water production rates in initial ensemble

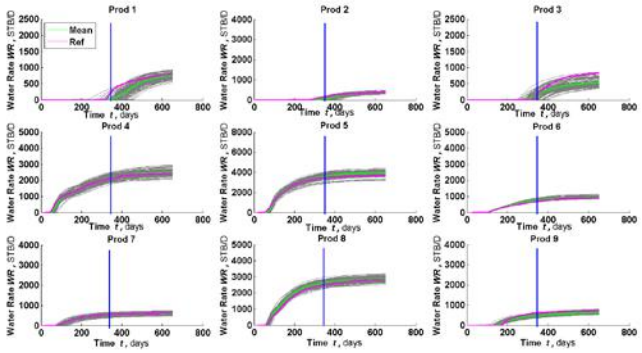

Figure 13. Water production rates in the third updated ensemble (GC-parameterization)

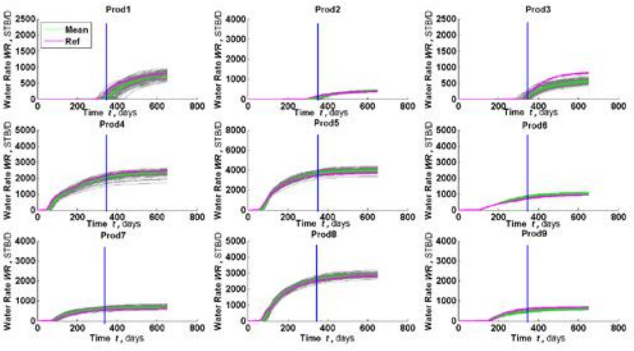

Figure 14. Water production rates in the third updated ensemble (FRM-parameterization)

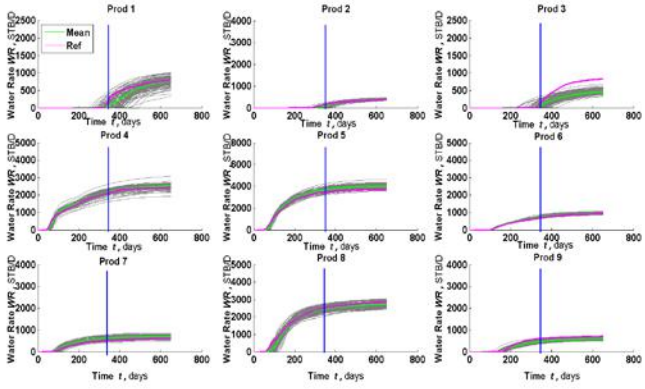

Figure 15. Water production rates in the third updated ensemble (RM-parameterization)

 Digital Object Identifier 10.32754/JMT.2022.1.01

In order to further analyze the comparison between the proposed parameterizations we compute in (16) the root mean square error (RMSE) using a weighted Euclidian distance between the reference, (*Ref*) and each ensemble member, X^i The RMSE is calculated for both the permeability field and the water production rates for a period of 651 days

$$RMSE^2 = \frac{\sum_{i=1}^{n_e}\sum_{j=1}^{n_d}\widehat{W_i}\left(V_j\left(Ref\right)-V_j\left(X^i\right)\right)^2}{n_d}, \qquad (16)$$

where n_d is the number of data, X^i denotes ensemble member number i, $\widehat{W_i}$ the corresponding likelihood weight and V_j is the variable of interests (i.e. the permeability and the total production rates). Table II presents the RMSE calculated for the permeability field and, in Table I, the RMSE calculated for total production rates for 651 days. Both tables indicate that, after three iterations, all parameterizations keep the values of RMSE within a small bandwidth and the parameterizations behave well. From the tables, we cannot rank the parameterizations based on the RMSE values (from the lowest to highest) of the updated ensembles because the differences between RMSE values in the updated ensembles are very small. However, from Table I, we can observe that the RMSE values of prior ensembles of RM-parameterization and FRM-parameterization in the second and third iterations are significantly higher than the RMSE of the GC-parameterization. This means that the resampling step from the training image yields prior ensembles of facies fields with a higher variability than for the GC-parameterization. We calculate the RMSE for the permeability, even though, in reality, the truth is not known. This indicator gives us some information about the quality of the estimation of the permeability field which, in this case, is similar to the facies field (we keep the permeability constant within facies). Here the behavior is the same as the one observed for total rates with the remark that the RMSE calculated from the updated ensemble of RM-parameterization has the smallest value. This indicates a better estimation of the true facies field.

TABLE I. RMSE CALCULATED FOR TOTAL RATES (STB/D)

	GC parameterization		**FRM parameterization**		**RM parameterization**	
	Initial	Updated	Initial	Updated	Initial	Updated
Iter 1	1085.58	264.26	1085.58	258.63	1085.58	301.98
Iter 2	369.15	194.48	694.85	177.98	583.87	254.05
Iter 3	365.25	159.34	482.52	144.65	454.67	164.56

TABLE II. RMSE CALCULATED FOR PERMEABILITY (MD)

	GC parameterization		**FRM parameterization**		**RM parameterization**	
	Initial	Updated	Initial	Updated	Initial	Updated
Iter 1	5.006	4.884	5.006	4.861	5.006	4.521
Iter 2	4.734	4.417	4.697	4.483	4.348	4.329
Iter 3	4.394	4.215	4.398	4.278	4.325	4.196

As a conclusion, we have observed that the data are equally matched by all parameterizations, but regarding the channel, the estimation has differences. All the parameterizations were able to detect the main features of the reference, but the GC-parameterization was not able to detect the connection that links the two main channels from the bottom of the reservoir. The RM-parameterization and FRM-parameterization were able to estimate it. Consequently, from the estimation perspective, the RM-parameterization gave an improvement.

VI. CONCLUSION

In this study, we have introduced two novel parameterizations of channelized reservoirs as extensions of a previous parameterization designed in the context of truncated Gaussian methodology (named gravity center, GC). In the GC-parameterization, the randomness of the parameter field was ensured only by the initial ensemble of the channelized reservoir; here we enhanced the randomness with a stochastic forcing involving the use of random numbers (seeds) as samples from a uniform distribution. For the first novel parameterization (named fully random mapping, FRM), we use for each ensemble member and each grid-cell different seed values when sampling from the conditional distribution. This choice destroys any spatial distribution of the parameter field. For the second parameterization (named random mapping, henceforth RM), we have used the same seed value for all grid-cells of an ensemble member; however the seeds are changed for different ensemble members. In this way, the parameter field keeps the same spatial dependence structure as the older parameterization but with higher prior variability. For the history matching part, we have used the iterative adaptive Gaussian mixture filter in three iterations for its ability to deal with highly nonlinear systems and for the resampling step between iterations. The results show that the spatial dependence structure is crucial in keeping the geological plausibility (realistic) during iterations. The facies fields of the updated ensembles of the FRM-parameterization are not keeping the multi-point geostatistics even after the third iteration. The uncontrolled use of the stochastic forcing does not help if we need an ensemble of updated facies realizations for the uncertainty quantification. From the estimation perspective, the random mapping parameterization was able to detect features that were not detected by the GC parameterization. The improvement is due to the higher prior variability, introduced by the use of different seeds when sampling from the conditional distribution. The data match and predictions were equally well estimated by all parameterizations.

REFERENCES

[1] J. Caers and T. Zhang, “Multiple-point geostatistics: a quantitative vehicle for integrating geologic analogs into multiple reservoir models” in Integration of Outcrop and Modern Analogs in Reservoir Modeling, AAPG MEMOIR, Jan. 01, 2004. doi: 10.1306/M80924C18.

[2] Y. Chang, A. S. Stordal, and R. Valestrand, “Integrated work flow of preserving facies realism in history matching: Application to the Brugge field”, *SPE Journal*, 21(4), Aug. 2016. doi:10.2118/179732-PA

[3] C. V. Deutsch and L. Wang, “Hierarchical object-based stochastic modeling of fluvial reservoirs”, *Mathematical Geology*, vol. 28, no. 7, pp. 857-880, 1996.

[4] O. Dorn and R. Villegas, “History matching of petroleum reservoirs using a level set technique”, *Inverse Problems*, vol. 24, no. 3: 035015, 2008. http://stacks.iop.org/0266-5611/24/i=3/a=035015.

[5] A. A. Emerick, “Investigation on principal component analysis parameterizations for history matching channelized facies models with

ensemble-based data assimilation", *Mathematical Geosciences*, 49(1), pp. 85-120, Jan. 2017. doi:10.1007/s11004-016-9659-5.

[6] A. A. Emerick and A. C. Reynolds, "Ensemble smoother with multiple data assimilation", *Computers & Geosciences*, 55, pp. 3-15, 2013. doi:10.1016/j.cageo.2012.03.011.

[7] G. Evensen, "The ensemble kalman filter: Theoretical formulation and practical implementation", *Ocean dynamics*, vol. 53, no. 4, pp. 343-367, 2003. doi:10.1007/s10236-003-0036-9.

[8] A. Galli, H. Beucher, G. Le Loc, B. Doligez, et al, "The pros and cons of the truncated gaussian method", *Geostatistical simulations*, pp. 217-233, Springer, 1994.

[9] R. Hanea, T. Ek and B. Sebacher, "Consistent Joint Updates of Facies and Petrophysical Heterogeneities Using an Ensemble Based Assisted History Matching", *Conference Proceedings, Petroleum Geostatistics*, 2015, Sep. 2015, cp-456-00015. doi:10.3997/2214-4609.201413598

[10] L. Hu, Y. Zhao, Y. Liu, C. Scheepens, and A. Bouchard, "Updating multipoint simulations using the ensemble Kalman filter", *Computers & Geosciences*, 51, pp. 7-15, 2013. doi:10.1016/j.cageo.2012.08.020.

[11] B. Jafarpour and M. Khodabakhshi, "A probability conditioning method (pcm) for nonlinear flow data integration into multipoint statistical facies simulation", *Mathematical Geosciences*, 43(2), pp. 133-164, 2011. doi:10.1007/s11004-011-9316-y

[12] B. Jafarpour and D. B. McLaughlin, "History matching with an ensemble Kalman filter and discrete cosine parameterization", *Computational Geosciences*, 12(2), pp. 227-244, 2008. doi:10.2118/108761-MS

[13] A. Journel, "Combining knowledge from diverse sources: An alternative to traditional data independence hypotheses", *Mathematical Geology*, 34(5), pp. 573-596, 2002.

[14] H. Jung, H. Jo, S. Kim, K. Lee, and J. Choe, "Recursive update of channel information for reliable history matching of channel reservoirs using EnKF with DCT", *Journal of Petroleum Science and Engineering*, 154, pp. 19-37, 2017, doi:10.1016/j.petrol.2017.04.016.

[15] K. Keogh and A. Martinius, "The development of fluvial stochastic modelling in the Norwegian oil industry: A historical review, subsurface implementation and future directions", *Sedimentary Geology*, 202(1{2), pp. 249-268, 2007. doi: https://doi.org/10.1016/j.sedgeo.2007.05.009

[16] M. M. Khaninezhad and B. Jafarpour, "A discrete imaging formulation for history matching complex geologic facies". *In SPE-182727-MS, SPE Reservoir Simulation Conference*, 20-22 Feb., Montgomery, Texas, USA. SPE, Society of Petroleum Engineers, 2017. doi:10.2118/182727-MS.

[17] M. M. Khaninezhad, B. Jafarpour, and L. Li, "Sparse geologic dictionaries for subsurface flow model calibration: Part I. inversion formulation", *Advances in Water Resources*, 39, pp. 106-121, 2012, doi:10.1016/j.advwatres.2011.09.002

[18] S. Krishnan, A. Boucher, and A. G. Journel, "Evaluating information redundancy through the tau model", *In Geostatistics Banff*, pp. 1037-1046, Springer, 2005.

[19] R. J. Lorentzen, K. M. Flornes, and G. Naevdal, "History matching channelized reservoirs using the ensemble kalman filter", *SPE Journal*, 17(1), pp. 137-151, 2012. doi:10.2118/143188-PA

[20] J. Ping and D. Zhang, "History matching of channelized reservoirs with vector-based level-set parameterization", *SPE Journal*, 19(3), pp. 514-529, 2014, doi:10.2118/169898-PA

[21] P. Sarma, L. J. Durlofsky, and K. Aziz, "Kernel principal component analysis for efficient, differentiable parameterization of multipoint geostatistics", *Mathematical Geosciences*, 40(1), pp. 3-32, 2008, doi:10.1007/s11004-007-9131-7.

[22] B. Sebacher, R. Hanea and A. Heemink, "A probabilistic parametrization for geological uncertainty estimation using the ensemble Kalman filter (EnKF)", *Computational Geosciences*, 17, pp. 813–832, 2013, doi:10.1007/s10596-013-9357-z.

[23] B. Sebacher, R. Hanea and A. Stordal," An adaptive pluri-Gaussian simulation model for geological uncertainty quantification", *Journal of Petroleum Science and Engineering*, 158, pp. 494-508, 2017. doi:10.1016/j.petrol.2017.08.038.

[24] B. Sebacher, A. Stordal, and R. Hanea, "Bridging Multi Point Statistics and Truncated Gaussian Fields for Improved Estimation of Channelized Reservoirs with Ensemble Methods", *Computational Geosciences*, 19(2), pp. 341-369, 2015, doi:10.1007/s10596-014-9466-3.

[25] B. Sebacher, A. Stordal, and R. Hanea, "Complex geology estimation using the iterative adaptive Gaussian mixture filter", *Computational Geosciences*, 20(1), pp. 133-148, 2016. doi: 10.1007/s10596-015-9553-0.

[26] B. Sebacher and R. Hanea, "Channelized reservoir estimation using a low-dimensional parameterization based on high-order singular value decomposition", *Computational Geosciences*, 24, pp. 509-531, 2020. doi:10.1007/s10596-019-09856-1

[27] B. Sebacher, R. Hanea and T. Ek, "Quantifying the Uncertainty in the Facies Probability Cubes Using an Ensemble Kalman Filter Methodology", *Conference Proceedings, Petroleum Geostatistics* 2015, Sep 2015, cp-456-00047. doi:10.3997/2214-4609.201413630.

[28] B. Sebacher, A. Stordal, and R. Hanea, "Different Parameterizations of the Initial Ensemble for a Channelized Reservoir in an Assisted History Matching Context", *Conference Proceedings ECMOR XV - 15th European Conference on the Mathematics of Oil Recovery*, Aug. 2016, cp-494-00079. doi:10.3997/2214-4609.201601817

[29] A. Stordal and R. Lorentzen, "An iterative version of the adaptive gaussian mixture filter", *Computational Geosciences*, 18(3), pp. 579-595, 2014. doi:10.1007/s10596-014-9402-6.

[30] A. Stordal H. A. Karlsen, G. Naevdal, H. J. Skaug, and B. Valles, "Bridging the ensemble Kalman filter and particle fillters: the adaptive gaussian mixture filter", *Computational Geosciences*, 15(2), pp. 293-305, 2011. doi:10.1007/s10596-010-9207-1

[31] S. Strebelle, "Conditional simulation of complex geological structures using multiple-point statistics", *Mathematical Geology*, 34(1), pp. 1-21, 2002.

[32] R. Tavakoli and A. C. Reynolds, "Monte carlo simulation of permeability fields and reservoir performance predictions with svd parameterization in rml compared with EnKF". *Computational Geosciences*, 15(1), pp. 99-116, Jan. 2011. doi:10.1007/s10596-010-9200-8.

[33] H. X. Vo and L. J. Durlofsky, "A new differentiable parameterization based on principal component analysis for the low-dimensional representation of complex geological models", *Mathematical Geosciences*, 46(7), pp. 775-813, Oct. 2014. doi:10.1007/s11004-014-9541-2.

[34] H. X. Vo and L. J. Durlofsky, "Data assimilation and uncertainty assessment for complex geological models using a new PCA-based parameterization", *Computational Geosciences*, 19(4), pp. 747-767, 2015. doi:10.1007/s10596-015-9483-x

[35] Y. Zhang, D. Oliver, Y. Chen, and H. Skaug, "Data assimilation by use of the iterative ensemble smoother for 2D facies models", *SPE Journal*, 20(1), pp. 169-185, 2015. doi:10.2118/170248-PA.

[36] Y. Zhao, F. Forouzanfar, and A. C. Reynolds, "History matching of multi-facies channelized reservoirs using ES-MDA with common basis DCT", *Computational Geosciences*, 21, pp. 1343–1364, 2017. doi:10.1007/s10596-016-9604-1.

[37] H. Zhou, L. Li, H.-J. H. Franssen, and J. J. Gomez-Hernandez, "Pattern recognition in a bimodal aquifer using the normal-score ensemble kalman filter", *Mathematical Geosciences*, 44(2), pp. 169-185, 2012. doi:10.1007/s11004-011-9372-3.